VNU Journal of Science: Natural Sciences and Technology

Journal homepage: https://js.vnu.edu.vn/NST

Original Article

One-step Synthesis of Sodium Hydroxide-assisted Hydrochar from Spent Coffee for Enhanced Adsorption Performance

Hoang Phuong Linh, Nguyen Quang Huy, Phan Tuan Ngoc*

VNU University of Science, 19 Le Thanh Tong, Hoan Kiem, Hanoi, Vietnam

Received 15th May 2025
Revised 25th August 2026; Accepted 08th October 2026

Abstract: Modification is a common method to enhance the physicochemical properties of hydrochar. In this work, hydrochar was synthesized from spent coffee grounds (SCG) with the presence of NaOH during the hydrothermal treatment in a one-step process. The adsorption of methylene blue (MB) in aqueous solution using SCG, SCG-derived hydrochar (HC-W), and NaOH-activated hydrochar (HC-S) as adsorbents was studied. The results showed that hydrochar can effectively remove MB with a high removal rate of above 90%. Among these materials, HC-S exhibited the highest MB adsorption capacity and the shortest time to reach the adsorption equilibrium. The MB adsorption kinetics and isotherm of hydrochar were well fitted by the pseudo-second-order kinetic model and the Langmuir model, respectively. The maximum adsorption capacity of HC-S for MB was 30.17 mg/g. The synergic effect between hydrothermal carbonization and NaOH activation plays a crucial role in enhancing hydrochar adsorption performance, which is favorable for the adsorption of MB onto the surface of hydrochar.

Keywords: Hydrochar; Activation; NaOH; One-pot synthesis.

1. Introduction

Organic dyes commonly exist in the wastewater from chemical industries such as textiles, plastics, ceramics, paper, and cosmetics [1-3]. It is well known as highly toxic, carcinogenic, teratogenic, and mutagenic contaminants, leading to serious environmental pollutants and health threats [4]. Thus, removing dyes in wastewater before discharge is an urgent issue that should be solved. Numerous techniques have been developed for the removal of dyes in wastewater, including adsorption, catalytic degradation, membrane separation, and oxidation [5-7]. Among these approaches, adsorption has been considered the most promising method because of its simplicity, easy operation, high efficiency, and low cost [8, 9]. The adsorption efficiency is significantly affected by the adsorbent materials.

Biomass-derived carbon materials are widely utilized as adsorbents due to their high specific surface area, versatile structural modification, and environmental friendliness [10]. Biomass sources are commonly

* Corresponding author.
E-mail address: tuanngocphan@hus.edu.vn

https://doi.org/10.25073/2588-1140/vnunst.5897

transferred to carbon materials by a pyrolysis process at high temperature in an inert environment, called biochar. However, the production of biochar involves a high energy consumption and greenhouse gas emission, limiting its application [11, 12]. Hydrochar, a carbon-based material prepared by hydrothermal carbonization of biomass, is considered an effective alternative material for biochar. Hydrochar possesses low energy demand, low gas emission, and numerous oxygen-containing functional groups on its surface [13]. Cavali et al., conducted the hydrothermal treatment of pine residual sawdust at 250 °C for 1 hour, producing hydrochar with the specific surface area of 30.94 m^2/g and pore volume of 0.143 cm^3/g [14]. Amado-Fierro et al. synthesized hydrochar with a specific surface area in a range of 2.5-9 m^2/g from five common waste types: organic fraction of municipal solid waste, green waste, grape bagasse, wood waste, and cheese whey [15]. The low porosity and uneven particle size distribution of hydrochar should be improved to increase the adsorption capacity for dyes [16].

The morphological structure and surface properties of hydrochar can be significantly enhanced through the modification process using either physical or chemical methods to improve its adsorption performance [17-19]. Physical modification is carried out at high temperature using mild oxidizing gases for a long time of heat treatment [20]. Thus, chemical activation has been considered a common method to boost the adsorption performance of hydrochar [21-23]. The chemical activation process can be conducted in two ways. One is one-step synthesis, in which the chemical regents are directly mixed with biomass during the hydrothermal process. The other is a two-step synthesis, where hydrochar is completely prepared, followed by the immersion of hydrochar in the chemical regent solution. Hydrochar can either be used directly after the activation or further carbonized at high temperature. Zhou et al., prepared activated hydrochar with NaOH 1.5 M after hydrothermal treatment [24]. The specific surface area of the activated hydrochar is twice as high two time of hydrochar prepared with the activation process. It led to the high maximum adsorption capacity for methylene blue (MB) of 357 mg/g. Rice straw-derived hydrochar was activated with K_2CO_3 and KOH solution through a two-step process by Babu's group [25]. The maximum adsorption capacity for MB increased from 111.65 to 434.63 mg/g after the activation process. It can be seen that the two-step synthesis is a complex process with higher energy consumption and excessive use of chemicals.

In this study, hydrochar material was synnthesized from spent coffee grounds (SCG) by a low-temperature, low-concentration, and one-step hydrothermal carbonization method with the presence of NaOH. The combination of NaOH activation and hydrothermal treatment in one pot further improves the porous structure and the adsorption performance of the as-synthesized hydrochars. The effects of adsorption time and MB solution concentration on the adsorption performance of hydrochars were investigated. Moreover, the adsorption equilibrium and kinetic characteristics were evaluated through fitting theoretical models to briefly elucidate the adsorption mechanism.

2. Experimental

2.1. Materials

The spent coffee ground was collected from the local coffee shop in Ha Noi, Viet Nam. Sodium hydroxide and anhydrous ethanol were purchased from Xilong (China). All chemicals were used directly without further purification.

2.2. Synthesis of Hydrochar

The spent coffee ground was sieved with a 100 mesh sieve, washed with deionized water (DW), and dried at 80 °C. The spent coffee ground was hydrothermally treated with different solvents (DW and NaOH solution). In

brief, dried spent coffee was added into DW or NaOH 0.05 M solution with a biomass to solution ratio of 1:1, followed by stirring at room temperature for 30 min. The mixture was transferred into a 100 mL Teflon liner autoclave and hydrothermally treated at 140 °C for 6 hours. Afterward, the suspension was separated from the liquid phase, cleaned with anhydrous ethanol and DW several times. The spent coffee-derived hydrochar was collected by centrifugation and dried at 80 °C for 12 hours. The hydrochars hydrothermally treated with DW and NaOH are recorded as HC-W and HC-S, respectively.

2.3. Characterization of Hydrochar

The surface morphology of hydrochar was observed by scanning electron microscopy (SEM). The chemical functional groups were determined by Fourier transform infrared (FT-IR, IRAffinity-1, Shimadzu, Japan). The X-ray diffraction (XRD) analysis was carried out with a D8 Advance (Brucker, Germany) equipment using copper Kα X-ray radiation at 40 kV and 40 mA. The N_2 adsorption-desorption measurement was conducted using TriStar II Plus (Micromeritics, United State). The specific surface area of hydrochar was determined by the Brunauer-Emmet-Teller (BET) method.

2.4. Batch Adsorption Experiments

The adsorption experiments were conducted in a 100 mL conical flask. In particular, 50 mg of hydrochar was shaken with 100 mL of 10 ppm MB solution for a given time at room temperature. After reaching the pre-set time, the concentration of the MB solution was identified from the calibration curve of the MB solution at 665 nm by a spectrophotometer (UV-Vis 722N Genius, Taisite, China). The adsorption capacity for MB at time t (min) was defined by Eq. (1):

$$q_t = \frac{(C_0 - C_t)}{m} V \qquad (1)$$

where q_t (mg/g) and C_t (mg/L) represented the adsorption capacity of hydrochar for MB and the MB concentration at time t (min), respectively; C_0 (mg/L) was the initial MB concentration; V (L) and m (g) were the solution volume and adsorbent dosage, respectively.

2.4.1. Kinetics Models for MB Adsorption

The effect of adsorption time (10, 20, 40, 60, and 100 min) was carried out for a kinetic study, while the mass of adsorbent was fixed at 50 mg. Lagergren pseudi-first order and pseudo-second order models were applied as Eq. (2) and (3) are described below, respectively.

$$\ln(q_e - q_t) = lnq_e - k_1 t \qquad (2)$$

$$\frac{t}{q_t} = \frac{1}{k_2 q_e^2} + \frac{1}{q_e} t \qquad (3)$$

where q_e (mg/g) is the equilibrium adsorption capacity; k_1 (1/h) and k_2 (g/mg.h) are the adsorption rate constants for pseudo-first order and pseudo-second order kinetics, respectively. The relationship between $\ln(q_e\text{-}q_t)$ versus t or t/q_t versus t was plotted according to the experimental data. The values of q_e, k_1, and k_2 were calculated based on the intercept and slope of the straight line.

2.4.2. Isotherm Models for MB Adsorption

MB adsorption experiments were conducted by adding 50 mg of adsorbent into 100 mL of MB solution with the different concentrations varied from 5 to 10 ppm for 90 min to investigate the adsorption isotherms. Langmuir and Freundlich isotherm models were investigated using the corresponding equations as follows:

$$\frac{C_e}{q_e} = \frac{1}{K_L q_m} + \frac{1}{q_m} C_e \qquad (4)$$

$$lnq_e = lnK_F + \frac{1}{n} lnC_e \qquad (5)$$

in which K_L (L/mg) is the Langmuir model constant; n (mg/g) and K_F $(mg/L)^{1/n}$ are Freundlich model constants; q_m (mg/g) is the maximum adsorption capacity. Plotting C_e/q_e against C_e or $\ln q_e$ against $\ln C_e$ based on the experimental data for identifying q_m, K_L, n, and

K_F constants by the intercept and slope of the straight line.

The reusability of hydrochar was performed by five times MB adsorption. After each experiment, hydrochar was collected by centrifugation, washed with ethanol and water several times, following by drying at 80 °C for next use.

3. Results and Discussion

3.1. Characterization

The SEM images of the spent coffee ground and hydrochar samples are shown in Figure 1. The SCG in Figure 1a displayed the agglomeration state of the particles with various sizes and shapes, indicating the low porosity. After hydrothermal treatment, the hydrochar possessed rough pores with homogeneous distribution on the surface, meaning a high specific surface area. However, numerous pores of HC-W were blocked and clogged by impurities, which may be carbon microspheres, forming from the polycondensation of cellulose, hemicellulose, and lignin during the hydrothermal process [26]. In contrast, the impurities were decomposed and removed from the pores of HC-S, producing rougher and clearer cracks and channels.

Besides the decomposition of the organic compounds in SCG, the presence of NaOH could release H_2, CO_2, and CO during the hydrothermal reaction [27]. It can improve the formation of pores in the hydrochar when these gases diffuse out of the surface of HC-S. These pores provided a larger contact surface and binding sites, which are favorable for the adsorption of MB on the surface of hydrochar. The surface area of hydrochar is enhanced by the hydrothermal process with NaOH.

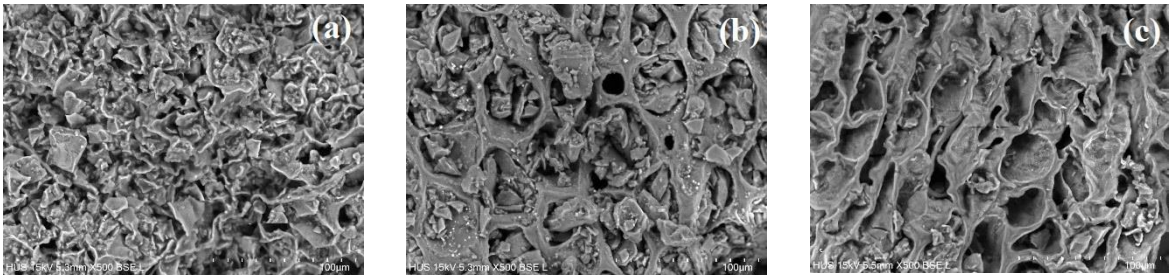

Figure 1. SEM image of (a) SCG, (b) HC-W, and (c) HC-S.

FT-IR spectra in Figure 2 indicated that the samples possessed several of oxygen-containing functional groups. A broad peak around 3400 cm^{-1} was attributed to the O–H stretching vibrations of hydroxyl or carbonyl groups [28]. These groups originally appeared in hemicellulose, cellulose, and lignin that were not completely decomposed after the hydrothermal treatment. The peaks observed in a range of 3000-2800 cm^{-1} represented asymmetric and symmetric stretching vibrations of aliphatic C–H [29]. The peak at around 1630 cm^{-1} was caused by C=C/C=O stretching vibrations [30, 31]. The –COOH bending vibration appeared at 1400 cm^{-1}. The band at 1075 cm^{-1} was assigned to C–O stretching vibration [30, 31]. After hydrothermal treatment, the strength of these functional groups in hydrochar was weaker than those in raw SCG. It indicated that a part of organic compounds, such as fatty acids and carboxylic acids in SCG, were decarboxylated during the hydrothermal process, resulting in the development of a porous structure and high specific surface area of hydrochar as well.

The XRD measurements were used to confirm the amorphous nature of hydrochar in the 2θ range of 10–70°. In Figure 2(b), a broad

peak at approximately 23° is attributed to amorphous carbon structure. There was no obvious difference between the samples before and after the hydrothermal treatment, which mean that the hydrothermal process did not change the phase structure of adsorbents.

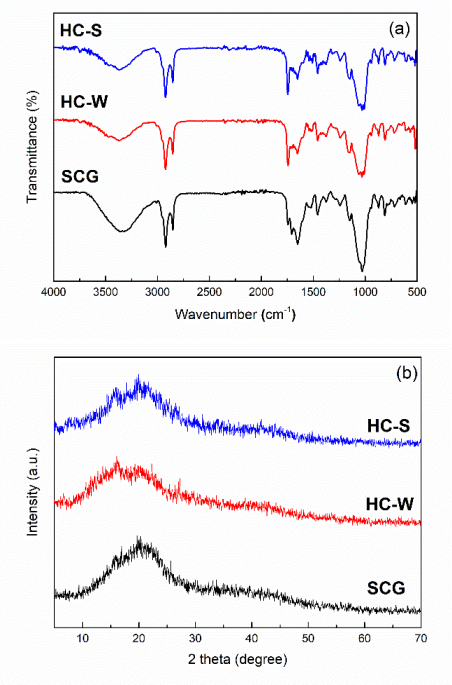

Figure 2. (a) FT-IR spectra and (b) XRD patterns of SCG, HC-W, and HC-S samples.

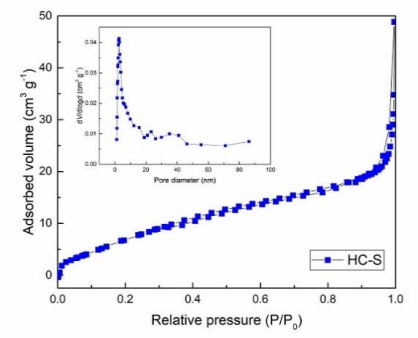

Figure 3. N_2 adsorption-desorption isotherm and pore size distribution (inset) of HC-S sample.

The N_2 adsorption-desorption isotherm of the HC-S sample in Figure 3 can be assigned as type IV isotherm with a distinct H3-type hysteresis loop at relative pressures between 0.45 and 1.0, according to UIPAC classification. It indicated that mesoporous structure exists in this sample. HC-S possessed a BET specific surface area of 33.06 m^2 g^{-1}. As shown in the inset figure, the material exhibited a narrow pore size distribution with a sharp peak centered at approximately 5 nm, confirming a predominantly mesoporous framework.

3.2. Adsorption Studies

The influence of contact time on MB adsorption performance for SCG and hydrochars was investigated, and the result is shown in Figure 4(a). All samples exhibited a similar tendency in the MB adsorption capacity. In particular, when the adsorption time was less than 40 min, these samples showed excellent MB adsorption capacity, which may come from sufficient adsorption active sites on the samples. The HC-S possessed the highest MB removal rate among the three samples, indicating the significant role of NaOH solution in the hydrothermal treatment process. As the adsorption time ranged from 40 to 100 min, the MB adsorption capacity moderately increased. The number of adsorption active sites decreased with increasing contact time due to the occupancy of MB, leading to an increase in MB diffusion resistance from the solution to the active sites. As a result, the MB adsorption capacity did not change after 100 min and gradually reached equilibrium. The MB equilibrium capacities of SGC, HC-W, and HC-S were 13.7, 17.5, and 18.4 mg/g at 100 min, respectively (Figure 4(b)).

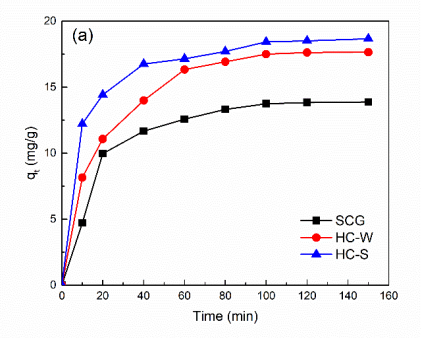

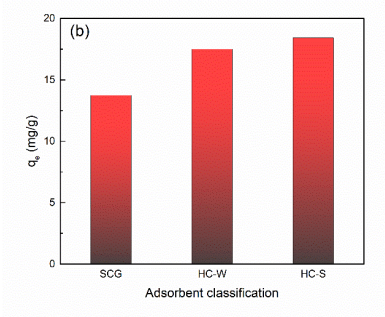

Figure 4. (a) Effect of adsorption time on MB adsorption capacity and (b) MB equilibrium adsorption capacity (absorbent dose 50 mg, MB solution 100 mL, 10 ppm, pH 7, room temperature).

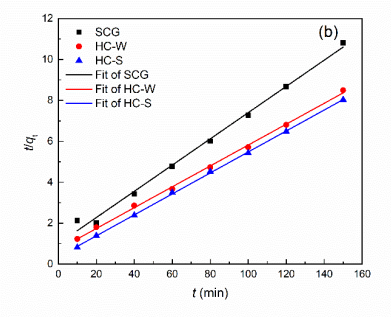

Figure 5. Kinetic fitting curves of (a) pseudo-first-order kinetics and (b) pseudo-second-order kinetics for hydrochars.

Figure 5 displays the MB adsorption kinetic fitting curves of SCG and hydrochars, and the corresponding fitting parameters are listed in Table 1. All samples exhibited a higher fitting degree for pseudo-second-order kinetics (R^2 > 0.994) than for pseudo-first-order kinetics (R^2 < 0.993). It indicated that the adsorption of SCG and hydrochar on the MB solution was a chemical process. The adsorption process was strongly influenced by the electron sharing and electron transfer between the functional groups of hydrochars and MB. In addition, the theoretical values of adsorption capacity at equilibrium calculated from the pseudo-second-order model were approximately similar to the experimental values. The HC-S showed the highest fitting constant k_2 among the three samples, demonstrating that HC-S took the shortest time to reach the adsorption equilibrium, which was in a well agreement with the experimental results.

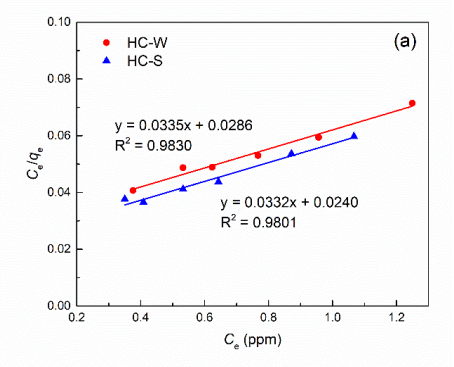

Figure 6. Linear fitting of (a) Langmuir model and (b) Freundlich model for hydrochars.

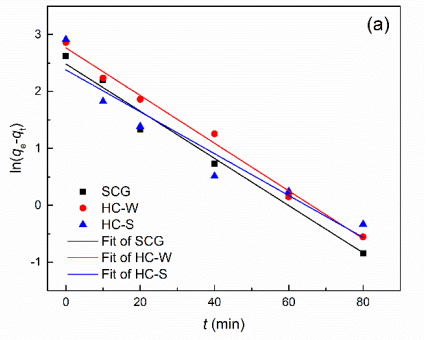

Figure 6 shows the linear fit of the Langmuir and Freundlich adsorption models of the hydrochars on the MB solution. The regression coefficients (R^2) of the Langmuir model were higher than those of the Freundlich model. It indicated that the adsorption of the MB solution on hydrochars mainly obeyed the

Langmuir model. The MB molecules monolayer on the hydrochar surface, and no intermolecular interaction exists. The fitting maximum adsorption capacity (q_m) calculated according to the Langmuir model was summarized in Table 1. HC-W and HC-S showed the q_m value of 29.89 and 30.17 mg/g, respectively, demonstrating that HC-S possessed a better adsorption performance for the MB solution than HC-W did. The appearance of NaOH in the hydrothermal treatment process facilitates the decomposition of impurities and the development of pore structure, which are favorable for the enhancement of adsorption performance.

The recycling of the hydrochar samples was perfomed by five runs of MB adsorption to evaluate the reusability. The results in Figure 7 showed a slightly decreased adsorption capacity (5%) after 5 cycles. It indicated the high stability and the excellent reusability of hydrochar for the MB adsorption.

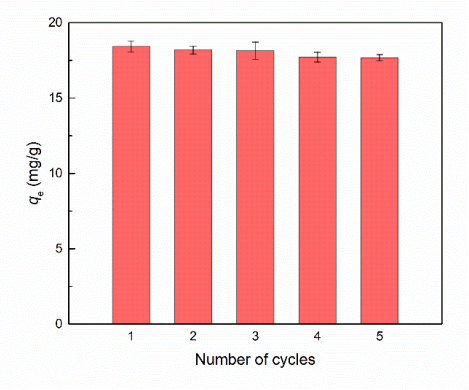

Figure 7. The regeneration performance of HC-S (absorbent dose 50 mg, MB solution 100 mL, 10 ppm, pH 7, room temperature).

Table 1. Fitting parameters of MB adsorption for SCG and hydrochars

Sample	Pseudo-first-order kinetics			Pseudo-second-order kinetics			Langmuir model			Freundlich model		
	q_e	k_1	R^2	q_e	k_2	R^2	q_m	K_L	R^2	K_F	1/n	R^2
SCG	12.00	0.0415	0.9787	15.61	0.0041	0.9942	-	-	-	-	-	-
HC-W	15.91	0.0419	0.9923	19.61	0.0036	0.9986	29.89	1.1710	0.9830	0.0620	0.4429	0.9669
HC-S	10.80	0.0368	0.9144	19.51	0.0074	0.9996	30.17	1.3811	0.9801	0.0562	0.4451	0.9457

4. Conclusion

In this study, the hydrochar was successfully prepared from spent coffee grounds by a one-step process, combining the hydrothermal carbonization and NaOH activation. The effect of synthesis conditions on the MB adsorption performance of hydrochar was investigated by controlling the adsorption time and the concentration of the MB solution. HC-S exhibited the highest MB removal rate (> 90%) and the maximum adsorption capacity of 30.17 mg/g. It may be due to the presence of NaOH in the hydrothermal process facilitates the development of a porous structure of hydrochar, increasing the specific surface area. In addition, the MB adsorption process for hydrochar was better described by the pseudo-second-order kinetics model and the Langmuir model, which is in good agreement with the experimental data.

Acknowledgements

The research is funded by Vietnam National University, Hanoi under project number QG.25.15.

References

[1] A. Haji, M. Naebe, Cleaner Dyeing of Textiles using Plasma Treatment and Natural Dyes: A Review, J. Cleaner Prod., Vol. 265, 2020, pp. 121866-121878, https://doi.org/10.1016/j.jclepro.2020.121866.

[2] B. Kamenicka, A Critical Review on Applications of Microreactors for the Treatment of Polluted Water with Organic Dyes, Sci. Total Environ., Vol. 969, 2025, pp. 178897-178906, https://doi.org/10.1016/j.scitotenv.2025.178897.

[3] K. F. Kayani, Mimetallic Metal-Organic Frameworks (BMOFs) for Dye Removal: A Review, RSC Adv., Vol 14, 2024, pp. 31777-31796, https://doi.org/10.1039/d4ra06626j.

[4] H. B. Slama, A. C. Bouket, Z. Pourhassan, F. N. Alenezi, A. Silini, H. Cherif-Silini, Diversity of Synthetic Dyes from Textile Industries, Discharge Impacts and Treatment Methods, Appl. Sci., Vol. 11, 2021, pp. 62555-622575, https://doi.org/10.3390/app11146255.

[5] H. Nawaz, M. Umar, A. Ullah, H. Razzaq, K. M. Zia, X. Q. Liu, Polyvinylidene Fluoride Nanocomposite Super Hydrophilic Membrane Integrated With Polyaniline-Graphene Oxide Nano Fillers for Treatment of Textile Effluents, J. Hazard. Mater., Vol. 403, 2021, pp. 123587-123599, https://doi.org/10.1016/j.jhazmat.2020.123587.

[6] B. L. Alderete, J. da Silva, R. Godoi, F. R. da Silva, S. R. Taffarel, L. P. da Silva, Evaluation of Toxicity and Mutagenicity of A Synthetic Effluent Containing Azo Dye after Advanced Oxidation Process Treatment, Chemosphere, Vol. 263, 2021, pp. 128291-128299, http://doi.org/10.1016/j.chemosphere.2020.128291.

[7] J. E. Gaayda, F. E. Tichou, R. Oukhrib, P. S. Yap, T. Q. Liu, M. Hamdani, Natural Flocculants for The Treatment of Wastewater Containing Dyes or Heavy Metals: A State-of-The-Art Review, J. Environ. Chem. Eng., Vol. 9, 2021, pp. 106060-106081, https://doi.org/10.1016/j.jece.2021.106060.

[8] O. A. B. Dahman, T. A. Saleh, Synthesis of Polyamide Grafted on Biosupport as Polymeric Adsorbents for the Removal of Dye and Metal Ions, Biomass Convers, Biorefin., Vol. 14, 2024, pp. 2439-2452, https://doi.org/10.1007/s13399-022-02382-8.

[9] H. M. M. N. Hazrin, A. Lim, C. Li, J. J. Chew, J. Sunarso, Adsorption of 2,4-Dichlorophenoxyacetic Acid onto Oil Palm Trunk-Derived Activated Carbon: Isotherm and Kinetic Studies at Acidic, Ambient Conditions, Mater. Today Proc., Vol. 64, 2022, pp. 1557–1562, https://doi.org/10.1016/j.matpr.2021.09.461.

[10] J. Wang, S. Wang, Preparation, Modification and Environmental Application of Biochar: A Review, J. Cleaner Prod., Vol. 227, 2019, pp. 1002–1022, https://doi.org/ 10.1016/j.jclepro.2019.04.282.

[11] A. U. Rajapaksha, S. S. Chen, D. C. W. Tsang, M. Zhang, M. Vithanage, S. Mandal, B. Gao, N. S. Bolan, Y. S. Ok, Engineered/Designer Biochar for Contaminant Removal/Immobilization from Soil and Water: Potential and Implication of Biochar Modification, Chemosphere, Vol. 148, 2016, pp. 276–291, https://doi.org/10.1016/j.chemosphere.2016.01.043.

[12] W. Yu, T. Ren, Y. Duan, S. Huai, Q. Zhang, Z. Cai, C. Lu, Mechanism of Al Toxicity Alleviation in Acidic Red Soil by Rice-Straw Hydrochar Application and Comparison with Pyrochar, Sci. Total Environ., Vol. 877, 2023, pp. 162849-162853, https://doi.org/10.1016/j.scitotenv.2023.162849.

[13] N. Chen, S. Cao, L. Zhang, X. Peng, X. Wang, Z. Ai, L. Zhang, Structural Dependent Cr (VI) Adsorption and Reduction of Biochar: Hydrochar Versus Pyrochar, Sci. Total Environ., Vol. 783, 2021, pp. 147084-147094, https://doi.org/10.1016/j.scitotenv.2021.147084.

[14] M. Cavali, H. Benbelkacem, B. Kim, R. Bayard, N. L. Junior, D. G. Domingos, A. L. Woiciechowski, A. B. C. Junior, Co-Hydrothermal Carbonization of Pine Residual Sawdust and Non-Dewatered Sewage Sludge – Effect of Reaction Conditions on Hydrochar Characteristics, J. Environ. Manage., Vol. 340, 2023, pp. 117994-118000, https://doi.org/10.1016/j.jenvman.2023.117994.

[15] A. A. Fierro, T. A. Centeno, J. L. R. Gallego, R. Forján, Critical Assessment of Biowaste-Derived Hydrochars for Remediating Contaminated Soils, Environ. Technol, Innovation, Vol. 38, 2025, pp. 104183-104195, https://doi.org/10.1016/j.eti.2025.104183.

[16] Y. Chen, S. A. Huang, K. Yu, J. Z. Guo, Y. X. Wang, B. Li, Adsorption of Lead Ions and Methylene Blue on Acrylate-Modified Hydrochars, Bioresour, Technol., Vol. 379, 2023, pp. 129067, https://doi.org/10.1016/j.biortech.2023.129067.

[17] M. Zulfajri, M. Adlim, N. Andalia, A. Rasool, S. Sudewi, G. G. Huang, Preparation of Magnesium Acetate-Modified Pineapple Crown Waste Hydrochar via Co-Hydrothermal Carbonization for a Specific Azo Dye Adsorption, Bioresour. Technol. Rep., Vol. 30, 2025, pp. 102127-102132, https://doi.org/10.1016/j.biteb.2025.102127.

[18] Z. Zhang, X. Rao, Q. Wu, S. Wang, Y. Chen, X. Yang, X. Sun, Q. Zhou, P. Lu, Preparationg of $FeCl_3$ Modified Wood Chips Hydrochar for Gas Phase Mercury Removal from Flue Gas, Fuel, Vol. 391, 2025, pp. 134802, https://doi.org/10.1016/j.fuel.2025.134802.

[19] K. Sathish, S. Saraswat, Screening and Characterization of Thermally Modified Biowaste-Derived Hydrochars for Slow-Release Fertilizer for Alkaline Soil Reclamation, Cleaner Waste Syst., Vol. 11, 2025, pp. 100257-100265, https://doi.org/10.1016/j.clwas.2025.100257.

[20] X. Zhang, W. Xiang, B. Wang, J. Fang, W. Zou, F. He, Y. Li, D.C.W. Tsang, Y.S. Ok, B. Gao, Adsorption of Acetone and Cyclohexane onto CO_2 Actived Hydrochars, Chemosphere, Vol. 245, 2020, pp. 125664-125672, https://doi.org/10.1016/j.chemosphere.2019.125664.

[21] J. Qu, F. Meng, F. Bi, Z. Jiang, M. Wang, Q. Hu, Y. Zhang, H. Yu, Y. Zhang, Nitrogen-Doped Porous Hydrochar for Enhanced Chromium (VI) and Bisphenol A Sscavenging: Synergistic Effect of Chemical Activation and Hydrothermal Doping, Environ. Res., Vol. 267, 2025, pp. 120667-120675, https://doi.org/10.1016/j.envres.2024.120667.

[22] Y. X. Gan, M. Yusuf, H. Ibrahim, Preparation and Characterization of Potassium Hydroxide Activated Hydrochar, Mater. Lett., Vol. 376, 2024, pp. 137328-137331, https://doi.org/10.1016/j.matlet.2024.137328.

[23] M. J. Lilian, R. Bissessur, K. Kang, Q. S. He, Y. Hu, Study of KOH-Activated Hydrochar for CO_2 Adsorption, J. Ind. Eng. Chem., Vol. 143, 2025, pp. 240-251, https://doi.org/10.1016/j.jiec.2024.08.026.

[24] F. Zhou, K. Li, F. Hang, Z. Zhang, P. Chen, L. Wei, C. Xie, Efficient Removal of Methylene Blue by Activated Hydrochar Prepared by Hydrothermal Carbonization and NaOH Activation of Sugarcane Bagasse and Phosphoric Acid, RSC Adv., Vol. 12, 2022, pp. 1885-1896, https://doi.org/10.1039/d1ra08325b.

[25] A. Rani, M. Rongpipi, A. Bhardwaj, K. Hussain, M. Arora, J.N. Babu, Improved Carboxylate Density Hydrochar by Alkylation of Surface Phenol for Adsorption of Cationic Dye in Aqueous Solution, Surf. Interfaces, Vol. 56, 2025, pp. 105511-105623, https://doi.org/10.1016/j.surfin.2024.105511.

[26] W. Yan, H. Zhang, K. Sheng, A. M. Mustafa and Y. Yu, Evaluation of Engineered Hydrochar from $KMnO_4$-Treated Bamboo Residues: Physicochemical Properties, Hygroscopic Dynamics, and Morphology, Bioresour. Technol., Vol. 250, 2018, pp. 806–811, https://doi.org/10.1016/j.biortech.2017.11.052.

[27] A. C. Martins, O. Pezoti, A. L. Cazetta, K. C. Bedin, D. A. S. Yamazaki, G. F. G. Bandoch, T. Asefa, J. V. Visentainer, V. C. Almeida, Removal of Tetracycline by NaOH-Activated Carbon Produced from Macadamia Nut Shells: Kinetic and Equilibrium Studies, Chem. Eng. J., Vol. 260, 2015, pp. 291–299, https://doi.org/10.1016/j.cej.2014.09.017.

[28] T. Zhang, X. Wu, S. M. Shaheen, Q. Zhao, X. J. Liu, J. Rinklebe, Ammonium Nitrogen Recovery from Digestate by Hydrothermal Pretreatment Followed by Activated Hydrochar Sorption, Chem. Eng. J., Vol. 379, 2020, pp. 122254-122267, https://doi.org/10.1016/j.cej.2019.122254.

[29] G. Prasannamedha, P. S. Kumar, R. Mehala, T. J. Sharumitha and D. Surendhar, Enhanced Adsorptive Removal of Sulfamethoxazole From Water Using Biochar Derived from Hydrothermal Carbonization of Sugarcane, J. Hazard. Mater., Vol. 407, 2021, pp. 124825, https://doi.org/10.1016/j.jhazmat.2020.124825.

[30] X. Xiao, B. Chen, L. Zhu, Transformation, Morphology, and Dissolution of Silicon and Carbon in Rice Straw-Derived Biochars under Different Pyrolytic Temperatures, Environ. Sci. Technol., Vol. 48, 2014, pp. 3411–3419, https://doi.org/10.1021/ es405676h.

[31] S. Fan, M. Zhao, J. Luo, W. Li, X. Fan, N. Zhou, H. Xu, Y. Shi, Facile Preparation of N/P Co-Doped Mesoporous Biochar for Efficient Removel of Methylene Blue from Aqueous Solutions: A 2D-FTIR-COS, Adsorption Mechanism Analysis, and Fixed-Bed Column Study, J. Water Process Eng., Vol. 72, 2025, pp. 107479, https://doi.org/10.1016/j.jwpe.2025.107479.